Functional analysis of GPx7 in non-alcoholic fatty liver disease

Hyeon Ju Kim

Department of Medical Science

The Graduate School, Yonsei University

Functional analysis of GPx7 in non-alcoholic fatty liver disease

Hyeon Ju Kim

Department of Medical Science

The Graduate School, Yonsei University

Functional analysis of GPx7 in non-alcoholic fatty liver disease

Directed by Professor Jae-woo Kim

The Master's Thesis
submitted to the Department of Medical Science
the Graduate School of Yonsei University
in partial fulfillment of the requirements for the degree of
Master of Medical Science

Hyeon Ju Kim

December 2019

This certifies that the Master's Thesis of

Hyeon Ju Kim is approved.

Thesis Supervisor : Jae-woo Kim

Thesis Committee Member #1 : Soo Han Bae

Thesis Committee Member #2 : Sungsoon Fang

The Graduate School

Yonsei University

December 2019

ACKNOWLEDGEMENTS

석사 학위논문을 마무리하며 도움을 주신 모든 분들께 감사의 인사를 드립니다.

먼저, 학위과정을 마치기까지 우여곡절의 순간이 많았지만 항상 믿고 부족한 저를 끝까지 이끌어 주신 김재우 교수님께 감사의 마음을 전합니다. 그리고 비록 많이 부족한 학위 논문이지만 좋은 결실을 맺을 수 있도록 실험에 관한 조언과 격려를 아끼지 않으신 배수한 교수님, 황성순 교수님, 그리고 생화학분자생물학교실의 김건홍 교수님, 박상욱 교수님, 허만욱 교수님, 윤호근 교수님, 전경희 교수님께도 감사의 말씀을 전합니다.

입학 후 여러 방면으로 어려움이 있을 때마다 마치 자신의 일처럼 옆에서 언제나 도움을 주고 격려해 주신 김효정 선생님 진심으로 감사합니다. 그리고 연구실에서 오랜 시간을 함께 보내며 많은 도움과 조언을 주신 조운 언니, 보경 언니, 요섭 오빠, 나희 언니, 규혜, 타티아나 그리고 혜민 언니, 다은 언니, 지윤 언니 모두 감사합니다. 더불어 생화학분자생물학 교실의 모든 교실원들에게 감사의 마음을 전하며, 많은 고민을 함께 나눠준 저의 동기 수빈이, 선호에게도 감사의 마음을 전하고 싶습니다.

마지막으로 항상 사랑으로 키워주시고 언제나 든든한 지원군이 되어주시며 부족한 저를 믿어주신 부모님께 감사의 말씀을 드립니다. 언제나 제 편이 되어 힘을 주시며 바르게 생각하고 행동할 수 있도록 가르쳐 주신 부모님께 자랑스러운 딸이 되기 위해 더욱 노력하겠습니다. 그리고 평생 저의 둘도 없는 친구이자 사랑하는 동생들 유진이, 용범이에게도 감사의 마음을 전합니다. 그리고 학위과정 동안 많은 의지가 되어준 저의 친구들도 고맙습니다. 앞으로 저는 새로운 전환점에 도달하겠지만, 이곳에서 배운 연구에 임하는 자세와 열정을 잊지 않고, 새로운 꿈과 비전을 향해 열심히 나아가겠습니다.

다시 한번, 저의 학위 과정에 도움을 주신 모든 분들께 감사드리며, 앞으로도 초심을 잊지 않고 감사하는 마음으로 모든 일에 최선을 다하겠습니다.

김현주 드림

TABLE OF CONTENTS

LIST OF FIGURES

LIST OF TABLE

ABSTRACT

Functional analysis of GPx7 in non-alcoholic fatty liver disease

Hyeon Ju Kim

Department of Medicine Science
The Graduate School, Yonsei University

(Directed by Professor Jae-woo Kim)

Non-alcoholic fatty liver disease (NAFLD) is one of the most common causes of chronic liver disease worldwide. NAFLD can progress to further irreversible liver failure such as non-alcoholic steatohepatitis (NASH) and cirrhosis. However, the molecular mechanisms involved in disease progression from simple steatosis to fibrosis remain poorly understood. This study aims to elucidate the molecular mechanisms that regulate the progression of NAFLD.

In this study, I analyzed RNA sequencing (RNA-seq) data to profile gene expression in simple steatosis and NASH-fibrosis model; cellular model (1) oleic acid (OA)-treated Hepa1-6 cells (murine hepatoma cell line), (2) transforming growth factor-β (TGF-β)-treated LX-2 cells (human stellate cell line) and mice model (3) simple steatosis of high-fat-diet (HFD)-fed mice liver (4) NASH-fibrosis of choline-deficient, L-amino acid-defined, high-fat-diet (CDAHFD)-fed mice liver. As a result of RNA-seq analysis, I found that glutathione peroxidase 7 (GPx7) expression was significantly increased in NASH-fibrosis compare to normal liver. So, I examined the role of GPx7 in cells. As a results, knockdown of the GPx7 expression using siRNA increased liver fibrosis and inflammation, whereas overexpression of GPx7 suppressed liver fibrosis and inflammation related gene expression in LX-2 cells. To determine whether GPx7 play a role *in vivo*, mice are fed CDAHFD for three weeks and a week before the sacrifice injected adenovirus containing short hairpin RNA (Ad-shRNA). As expected, knockdown of GPx7 induced liver fibrosis and inflammation as shown by masson's trichrome staining and plasma ALT and AST level, respectively. These results suggest that GPx7 may be a novel regulator of liver fibrosis. Oxidative stress has been implicated in the pathogenesis of NAFLD. To determine whether GPx7 is involved in oxidative stress regulation, I measured reactive oxygen species (ROS) production in GPx7 overexpressed LX-2 cells. As showing that overexpression of GPx7 reduced oxidative stress, thereby attenuated NASH. Taken together, these results

indicate that GPx7 can alleviate oxidative stress and prevent liver fibrosis, suggesting that activating GPx7 enzyme activity is a useful therapeutic strategy for NASH-fibrosis.

Key words: Hepatocytes, Metabolic disease, liver steatosis, Non-alcoholic fatty liver disease (NAFLD), Liver fibrosis, Non-alcoholic steatohepatitis (NASH), choline-Deficient, L-amino acid-defined, High-Fat-diet, Gene therapy

Functional analysis of GPx7 in non-alcoholic fatty liver disease

Hyeon Ju Kim

Department of Medicine Science
The Graduate School, Yonsei University

(Directed by Professor Jae-woo Kim)

I. INTRODUCTION

Non-alcoholic fatty liver disease (NAFLD) is one of the most common liver diseases[1]. NAFLD encompasses a spectrum of liver diseases, from simple steatosis to steatosis combined with varying degrees of inflammation and fibrosis[2]. The early stage of NAFLD is simple steatosis, it is defined as when the content of triglycerides in the liver is higher than 95% or the ratio of triglycerides in the cytoplasm is 5% in liver[3,4]. It is reversible via lifestyle

intervention, such as exercise[5] or caloric restriction[6]. Hepatic steatosis can be progress to non-alcoholic steatohepatitis (NASH), which can develop end-stage liver disease[2,3]. NASH shows pathological and fibrosis opinion such as ballooning degradation, cell death, inflammation and collagen accumulation[7]. There are several therapeutic agents for NASH such as Thiazolidinediones (TZDs)[8], Metformin[9], Vitamin E[10,11], but these induce a lot of side effect. So, specific therapeutics to treat NASH is needed.

Excessive fat accumulation in the liver induces oxidation and production of pro-inflammatory cytokines and adipokines (adiponectin, leptin, TNFα, IL-6)[3]. During liver injury HSCs are activated by transdifferentiation into a myofibroblastic phenotype (known as activated HSCs). Activated HSCs are highly fibrogenic and contractile, and thus play a major role in hepatic fibrosis. On the other hand, reactive oxygen species (ROS) was implicated to have an important role in activation and proliferation of HSCs[12].

Over the past decades, much effort has been focused on the role of oxidative stress in fibrogenesis[13,14]. Oxidative stress derived from hepatocyte injury can induce the elevation of transforming growth factor-β (TGF-β)[15]. TGF-β has been well documented to up-regulate the expression of collagen gene in the liver via the ROS[16]. Increased ROS levels can exacerbate the inflammatory responses by activating several pro-inflammatory signal pathways, such as MAPK, NF-κB and JAK-STAT[17-20]. Therefore, ROS can promote liver fibrogenesis either by directly activating HSCs resulting in increased collagen

production and deposition or by aggravating the inflammatory responses resulting in indirect enhancement of liver fibrosis[21].

In this study, I used Oleic acid (OA) treated Hepa1-6 cells (murine hepatoma cell line) and high-fat-diet (HFD)-induced simple steatosis mice liver as simple steatosis model. TGF-β treated LX-2 cells (human stellate cell line) and choline-Deficient, L-amino acid-defined, High-Fat diet (CDAHFD)-induced NASH-fibrosis mice liver as NASH-fibrosis model. Using these model system, I analyzed RNA sequencing (RNA-seq) to profile gene expression of simple steatosis and NASH-fibrosis. In this analysis, I found novel regulator Glutathione peroxidase 7 (GPx7) which can be therapeutics that target NASH-fibrosis. GPx7 expression was also highly detected in liver biopsies from patients with NASH-fibrosis.

GPx7 is a member of the glutathione peroxidase (GPx) family. GPx is the general name of enzyme family with peroxidase activity whose main biological role is to protect the organism from oxidative damage[22]. So far, eight different isoforms of GPx (GPx1-8) have been identified in human. GPx7 an intracellular antioxidant enzyme responsible for reducing peroxidized phospholipids. The phenotypes associated with GPx7 deficiency in mouse or human including ROS accumulations, auto-immune disorders, and obesity are also revealed[23]. However, GPx7 has not been reported to be associated with NAFLD through ROS regulation.

In this study, I found that GPx7 is highly expressed in NASH-fibrosis and

is a novel regulator of NASH-fibrosis. The expression of GPx7 is enriched in TGF- β treated LX-2 cells and CDAHFD fed mice liver. These observation suggest that GPx7 plays a critical role in NASH-fibrosis. I also demonstrated that GPx7 affects oxidative stress via decreasing active oxygen. Taken together, these findings suggest that GPx7 can represent a novel therapy for treatment of NASH-fibrosis.

II. MATERIALS AND METHODS

1. Experimental animals

Male C57BL/J mice were purchased from the Japan SLC (Shinzuoka, Japan). The animals were maintained in a temperature-controlled room (22 °C) on a 12:12-hrs light-dark cycle. Six-week-old mice were fed a normal chow-diet for normal liver model, and CDAHFD (Choline-Deficient, L-amino acid-defined, High-fat diet, Research Diets, New Brunswick, NJ, USA) for 3 wks for NASH-fibrosis liver model. Eight-week-old male C57BL/6 mice were injected with adenoviral containing short hairpin RNA (shRNA) or control recombinant adenovirus. Recombinant adenovirus (1×10^9 pfu) were delivered by tail-vein-injection. After seven days, mice are sacrificed, securing the liver. All procedures were approved by the Committee on Animal Investigations of Yonsei University.

2. Cell culture

Hepa1-6 cells (murine hepatoma cell line) and LX-2 cells (human stellate cell line) is different fraction cells in liver. Hepa1-6 cells were purchased form the American Type Culture Collection (Manassas, Virginia, USA). Hepa1-6 cells were maintained Dulbecco's Modified Eagle Medium: Nutrient Mixture F-12 (DMEM/F12; Invitrogen, Carlsbad, CA, USA) containing 100 U/ml penicillin, 100 mg/ml streptomycin, supplemented with heat-inactivated 10%

fetal bovine serum (FBS; Invitrogen) at 37 °C, in an atmosphere of 95% air and 5% CO_2. And LX-2 cells were maintained Dulbecco's Modified Eagle Medium (DMEM; Invitrogen) containing 100 U/ml penicillin, 100 mg/ml streptomycin, supplemented with heat-inactivated 10% FBS at 37 °C, in an atmosphere of 95% air and 5% CO_2.

3. Staining analysis

Oil red-O (ORO) staining is used to observe lipid accumulation in cells. And Picro-Sirius Red Staining is used to observe fibrosis, it is stained collagen to red, muscle fiber and cytosol to yellow. For ORO staining, cells were washed once in phosphate-buffered saline (PBS) and fixed with 3.7% formalin in PBS for 5 min, rinsed with distilled water. The staining solution was prepared by dissolving 0.5 g oil red-O (Sigma, St.Louis, MO, USA) in 100 ml of isopropanol; 6 ml of this solution was mixed with 4ml of distilled water, and filtered. The fixed cells were stained with staining solution for 1 hr. The staining solution was removed and cells were rinsed twice with distilled water. For Picro-Sirius Red Staining, cells were washed once in distilled water, and the staining solution was applied to completely cover the tissue section and incubated for 60 min. The staining solution was removed and cells were rinsed twice with acetic acid solution and absolute alcohol.

4. Preparation of recombinant adenovirus

Murine GPx7 was obtained by reverse transcriptase-polymerase chain reaction (RT-PCR) with total RNA obtained from C57BL/6 mice. Recombinant adenovirus, containing the murine GPx7 gene under the control of the CMV promoter, was prepared. I first constructed an E1 shuttle vector expressing murine GPx7. The newly constructed E1 shuttle vector was then linearized with *Pme* I digestion. The linearized shuttle vector was then cotransformed into *Escherichia coli* BJ5183 along with pAdEasy1 vector. The virus was propagated in 293A cells and purified by CsCl density purification, dissolved in 1× PBS and stored at -80 ℃. Viral particle numbers were calculated from measurements of absorbance at 260 nm (A_{260}). The multiplicity of infection (MOI) was calculated from viral particle number. Recombinant adenovirus containing the GFP gene was used as a control.

5. Measurement of triglyceride amount in the hepatocytes

Lipid extracts were prepared by homogenizing 0.2 g of liver in chloroform/methanol (2:1, v/v) with a final volume of 4 ml. The homogenate was incubated with vortexing for 10 min, then 0.8 ml of 50 mM NaCl was added, vortexed for 10 min, and then centrifuged at 4°C for 10 min. The organic phase (25 μl of lower layer) was transferred and 25 μl of Triton X-100/chloroform (7.5:17.5, v/v) was added into samples and vortexed for 10 min. The solvents were vaporized with a vacuum evaporator. TG concentrations were determined using 25 μl of extract in a commercial colorimetric assay

(Thermo scientific, Waltham, MA, USA). Samples and standards were vortexed and incubated at 37 °C for 30 min, and TG level were calculated from measurements of absorbance at 500 nm and expressed as mg TG/g liver wet weight.

6. Histological analysis

The liver tissues were fixed in 10% neutral-buffered formalin. Following fixation, the liver was trimmed, embedded in cryo block, sectioned, and stained with hematoxylin and ecosin (H&E) and masson's trichrome.

7. Gene expression analysis

Total RNA was isolated using TRIzol reagent (Invitrogen, Carlsbad, CA, USA) according to the manufacturer's instructions. For RT-PCR, cDNA was synthesized from 5 μg of total RNA using random hexamer primers and Superscript reverse transcriptase III (Invitrogen). Real-time PCR were conducted using SYBR Green Master mix (Applied Biosystems, Foster city, CA, USA) in a total volume of 20 μl. Transcripts were detected by Real-time qPCR with a Step One instrument (Applied Biosystems). All data were normalized to 18s and quantitative measures, and were obtained using the ΔΔ-Ct method. All reactions were perfomed in duplication. Primer pairs for specific target genes were disigned according to Table 1. All reactions were

performed in duplicate. Relative expression levels and s.d. values were calculated using comparative method.

8. Transient transfection assay and siRNA

Cells were plated into 60-mm diameter dishes 24 hrs before transfection. The following double-stranded stealth siRNA oligonucleotides (Santa Cruz Biotechnology, Dallas, TX, USA) were used: mouse GPx7 siRNA oligonucleotides (sc-145747), human GPx7 siRNA oligonucleotides (sc-78832). Control oligonucleotides with comparable GC content were also from Invitrogen. For knockdown, cells were transfected with control or gene-specific siRNA at 60 nM in OPTI-MEM medium using Lipofectamine RNAiMAX (Invitrogen, Carlsbad, CA, USA), according to the manufacture's protocol. The next day, the medium was replaced with fresh DMEM containing 10% FBS, 100 U/ml penicillin and 100 ug/ml streptomycin, and the cells were incubated for 24 h before harvest. Total RNA extracts were prepared from the cell at the indicated time point (2 days), and RT-PCR or Real-time PCR were performed. For the overexpression, the cells were plated at a density of 5×10^5 cells/well. The plasmid, GPx7 overexpressing vector (pcDNA3-GPx7-FLAG) was packaged with Lipofectamine 2000 (Invitrogen), and cells were transfected with either a control or GPx7-overexpressing vector according to the manufacturer's instructions.

9. Western blot analysis and antibodies

For protein analysis, cells were washed with PBS and lysed in a buffer containing 1 % sodium dodecyl sulfate (SDS) and 60 mM Tris-Cl, pH 6.8, and tissues were lysed in PRO-PREP™ (iNtRON Biotechnology, Seoul, KOREA). The lysate was mixed briefly using a vortex, boiled for 10 min, and centrifuged at 13,000 g for 10 min at 4 °C. Protein concentrations were assessed using the BCA assay kit (Pierce, Waltham, MA, USA). Protein samples of equal amount were separated by SDS-PAGE and transferred to nitrocellulose membranes. Immunoblot analysis were performed using the following antibodies: polyclonal antibody against GPx7 (Proteintech, Rosemont, IL, USA), Col1a1 (Abcam, Cambridge, UK), TNFα (Cell Signaling, Deavers, MA, USA), αSMA, TIMP1, MMP13, ADRP, and GAPDH (Santa Cruz Biotechnology, Dallas, TX, USA).

10. Statistical analysis

All results are expressed as mean ± s.d. Statistical comparisons of groups were made using an unpaired Student's test.

Table 1. Sequences of oligonucleotide primers used for quantitative real time PCR (qPCR)

Oligonucleotide		Sequence (5' → 3')
GPx7	Sense Antisense	AGG AAC CAG ACA CCA ACA GG CCG TCT GGG TCC ACT AGG TA
GPx7 (Human)	Sense Antisense	ACT GGT GTC GCT GGA GAA GT GTT GCT GTC AGG CTC CTG TT
TGF-β	Sense Antisense	GCC TGA GTG GCT GTC TTT TGA GGC TGA TCC CGT TGA TTT CCA
TGF-β (Human)	Sense Antisense	CCC AGC ATC CTG CAA AGC TC GTC AAT GTA CAG CTG CCG CA
COL1a1	Sense Antisense	CGA GTC ACA CCG GAA CTT GG GGC ACC AAT GTC CAA GGG AG
COL1a1 (Human)	Sense Antisense	GTG CTA AAG GTG CCA ATG GT CTC CTC GCT TTC CTT CCT CT
αSMA	Sense Antisense	CAC CAA CTG GGA CGA CAT GG GCC TTA GGG TTC AGT GGT GC
αSMA (Human)	Sense Antisense	AAA AGA CAG CTA CGT GGG TGA GCC ATG TTC TAT CGG GTA CTT C
TIMP1	Sense Antisense	CCC CAG AAA TCA ACG AGA CCA GGC CCG TGA TGA GAA ACT CTT
TIMP1 (Human)	Sense Antisense	ACC TGC AGT TTT GTF GCT CC CGG GAC TGG AAG CCCC TTT TC

PAI-1	Sense Antisense	CCT CCT CAT CCT GCC TAA GTT ACC TCG ATC CTG ACC TTT TGC
PAI-1 (Human)	Sense Antisense	CGC CAG AGC AGG ACG AA CAT CTG CAT CCT GAA GTT CTC A
TNFα	Sense Antisense	CCA GGC GGT GCC TAT GTC TC CAG CCA CTC CAG CTG CTC CT
TNFα (Human)	Sense Antisense	GAA AGC ATG ATC CGG GAC GTG GAT GC AGA GAG GAG GTT GAC
IL-1β	Sense Antisense	CCT GGG CTG TCC TGA TGA GA CTG CCA CAG CTT CTC CAC AG
IL-1β (Human)	Sense Antisense	CGA TCA CTG AAC TGC ACG CT TCT CC GCT GTA GAG TGG GC
ADRP	Sense Antisense	CAG ACT GTC CTG GTC AAC GC TGC TAG ATG TGA GGA GCG CA
ADRP (Human)	Sense Antisense	AAA GGC ATT GGC TGG AAG AA TCC TCT GAC ATT TGC AGG TCT ATC
GAPDH	Sense Antisense	AGG TCG GTG TGA ACG GAT TTG- TGT AGA CCA TGT AGT TGA GGT CA
GAPDH (Human)	Sense Antisense	GGA GCG AGA TCC CTC CAA AAT GGC TGT TGT CAT ACT TCT CAT GG

III. RESULTS

1. GPx7 is highly expressed in Non-alcoholic fatty liver disease

A previous report established the simple steatosis and fibrosis model *in vitro* and *in vivo*[24]. Simple steatosis was induced in the oleic acid (OA)-treated Hepa1-6 cells *in vitro* and high-fat-diet *in vivo*. And NASH-fibrosis was promoted in transforming growth factor-β (TGF-β)-treated LX-2 cells *in vitro* and CDAHFD *in vivo*. The reason for establishing the *in vitro* and *in vivo* models for mimicking steatosis and NASH-fibrosis was to select the novel genes that increase or decrease at the same time in three models by adding the human database; in a collaboration with Dr. Kim Won (Boramae Hospital, Seoul National University).

To find the novel regulator of NAFLD, I analyzed RNA-seq database. As a result, I selected meaningful genes which are expressed more than five-fold higher in NAFLD (Figure 1A). Although several genes were detected, because only GPx7 was highly expressed in human biopsy, I focused on GPx7 (Figure 1C). To gain insight into the biological activity of GPx7, I first examined its expression profile in simple steatosis and NASH-fibrosis (Figure 1B). The expression of GPx7 in simple steatosis was unchanged, but in NASH-fibrosis was highly increased. These data indicated that the expression of GPx7 increased in NASH-fibrosis model.

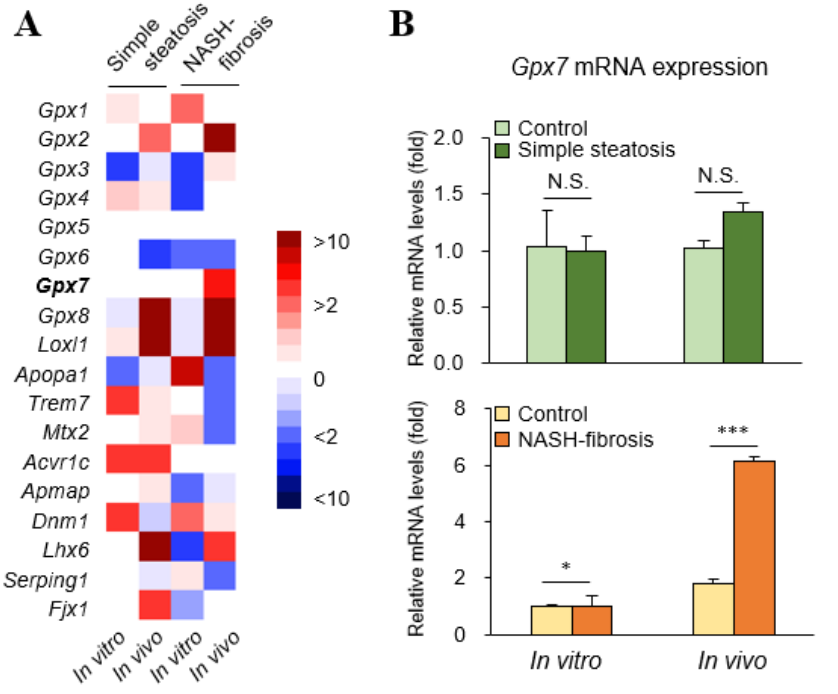

C

Gene_name	NAFLD_mean	Normal_mean	NAFLD (Human)
Gpx7	64.9	44.6	0.49

Figure 1. GPx7 is highly expressed in NASH-fibrosis. (a) Selected genes from RNA-seq. (b) Real-time PCR of *GPX7* expression in simple steatosis and NASH-fibrosis. (c) Normal_mean is GPx7 expression in normal liver patient liver biopsy, and NAFLD_mean is GPx7 expression in NAFLD patient liver biopsy. Human samples are received from Boramae Hospital, Seoul National University. All data are presented ± s.d. **P*<0.05, ***P*<0.01, ****P*<0.001.

2. GPx7 does not affect in Heap1-6 induced simple steatosis

In Figure 1, GPx7 did not increase the expression in simple steatosis. In order to determine that no change in expression of GPx7 did not affect simple steatosis at all, I explore the role of GPx7 in simple steatosis and performed knockdown of GPx7 in Hepa1-6 cells. Knockdown of GPx7 increased lipogenesis related genes such as perilipin-2 (ADRP) and cluster of differentiation 36 (CD36) (Figure 2A). However, ORO staining in siGPx7-treated Hepa1-6 cells showed a similar pattern compared to control (Figure 2B), indicating that GPx7 does not induce lipid accumulation. Next, I constructed overexpression vector to explore whether the forced expression of GPx7 can alter the pattern of lipid accumulation in Hepa1-6 cells. According to the UCSC database (genome.ucsc.edu), GPx7 is expressed in very low level in normal liver compared to other tissues; thus, I thought that overexpression of GPx7 may help analyzing a role of GPx7 in steatosis. Overexpression of GPx7 increased ADRP gene expression, but CD36 gene expression was unchanged compared to control (Figure 3A). Lipid droplets on ORO staining in GPx7 overexpressed Hepa1-6 cells also showed unchanged pattern compared to control. (Figure 3B). However, pro-inflammatory markers such as interleukin 1 beta (IL-1β), tumor necrosis factor alpha (TNFα) expression indicated increased levels in overexpression of GPx7 (Figure 3C). Moreover, the protein levels of lipogenic markers (ADRP and CD36) did not affect in GPx7-overexpressed Hepa1-6 cells (Figure 3D). Taken together, because the changes in lipogenesis

related markers expression according to GPx7 function in Hepa1-6 cells are inconsistent, I concluded that GPx7 did not effective role in simple steatosis.

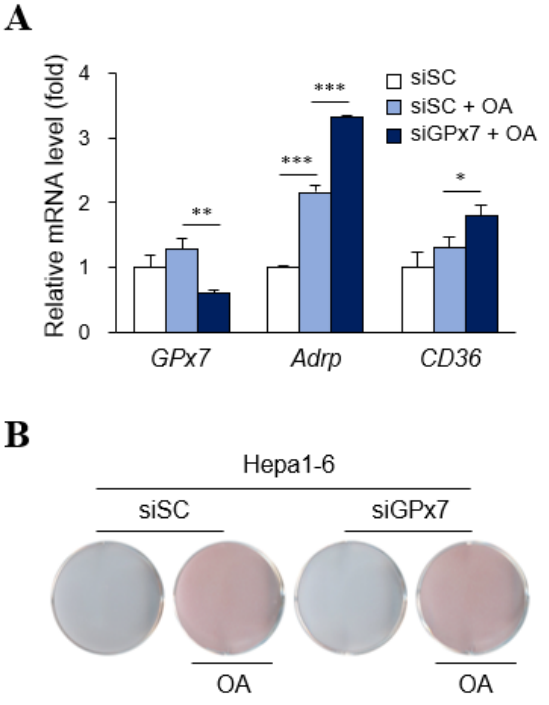

Figure 2. Knockdown of GPx7 does not induce TG accumulation in Hepa1-6 cells. (a) Relative mRNA expression of indicated genes in Hepa1-6 cells. Cells transfected with either negative control siRNA or si-GPx7 were treated with 600 mM OA. (b) Oil-Red-O staining in Hepa1-6 cells. All data are presented ± s.d. **P*<0.05, ***P*<0.01, ****P*<0.001.

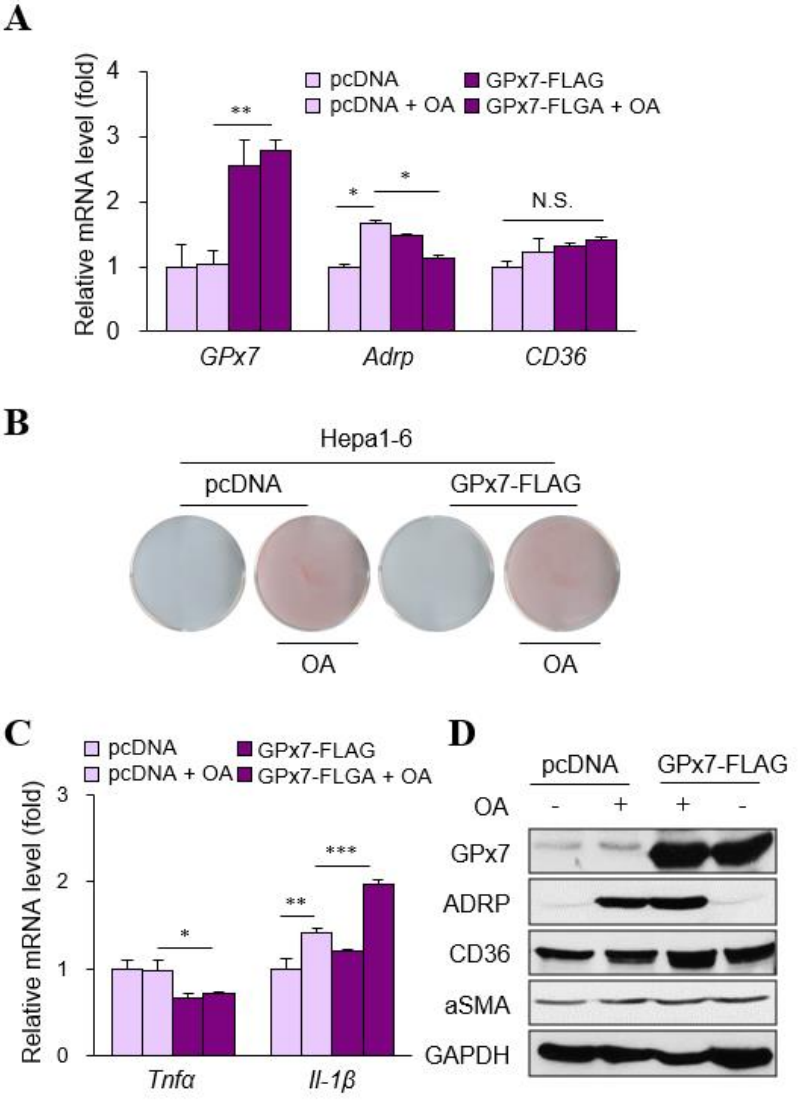

Figure 3. Overexpression of GPx7 does not affact in Hepa1-6 cells. (a) Relative mRNA expression of indicated genes in Hepa1-6 cells. Cells transfected with the pcDNA3.0 or pcDNA3-GPx7-FLAG vector. (b) Oil-Red-O staining in Hepa1-6 cells. (c) Relative mRNA expression of indicated genes in Hepa1-6 cells. (d) Cells transfected with the pcDNA3.0 or pcDNA3-GPx7-FLAG vector. Western blotting analysis using indicated antibodies. GAPDH was used as loading control. All data are presented ± s.d. **P*<0.05, ***P*<0.01, ****P*<0.001.

3. GPx7 plays a critical role in hepatic stellate cells induced NASH-fibrosis

To explore the function of GPx7 in NASH-fibrosis, LX-2 cells were treated with TGF-β, which lead to HSCs activation. To determine the molecular mechanisms underlying the role of GPx7 , GPx7 is knocked down in LX-2 cells (Figure 4A). As shown in Figure 4A, C, liver fibrosis was significantly deterioated in GPx7-knockdown LX-2 cells as indicated by Picro-Sirius Red staining and real-time PCR analysis of fibrosis related genes. Moreover, pro-inflammatory markers expression also increased in GPx7 knockdown LX-2 cells (Figure 4B). These results suggest that knockdown of GPx7 increases TGF-β induced liver fibrosis in LX-2 cells. To examine gain-of-function of GPx7 in LX-2 cells, I constructed a GPx7 overexpressing vector for human sequence, transfected the plasmid into LX-2 cells. Overexpression of GPx7 reduced NASH-fibrosis and inflammation related gene expression (Figure 5A, B). Improved NASH-fibrosis was associated with a significant decrease in pro-fibrotic and pro-inflammatory marker expression in GPx7-overexpressing cells (Figure 5C). To investigate GPx7 regulates oxidative stress, I measured ROS production (Figure 5D). As expected, Overexpression of GPx7 suppressed ROS induction. These results suggest that GPx7 attenuates NASH-fibrosis reducing oxidative stress.

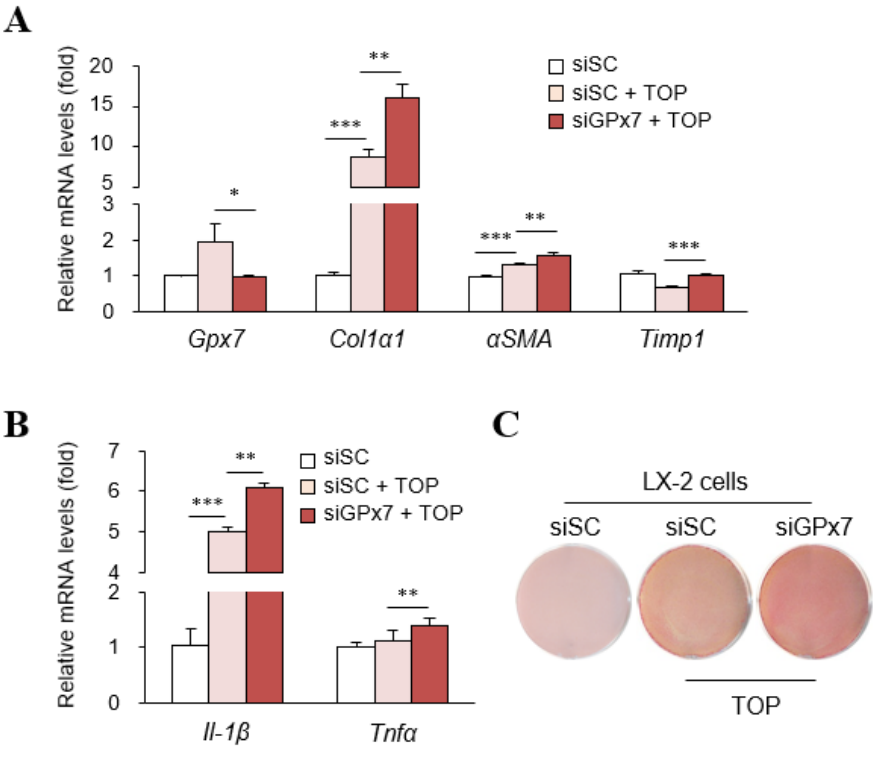

Figure 4. Knockdown of GPx7 induces hepatic fibrosis, inflammation related gene expression in LX-2 cells. (a, b) Relative mRNA expression of indicated genes in LX-2 cells. Cells transfected with either negative control siRNA or si-GPx7 were treated with TOP. TOP, TGF-β (3 ng) and FFA (1 mM OA, PA). (c) Sirus Red staining in LX-2 cells. Collagen, red; muscle fiber, yellow. All data are presented ± s.d. **P*<0.05, ***P*<0.01, ****P*<0.001.

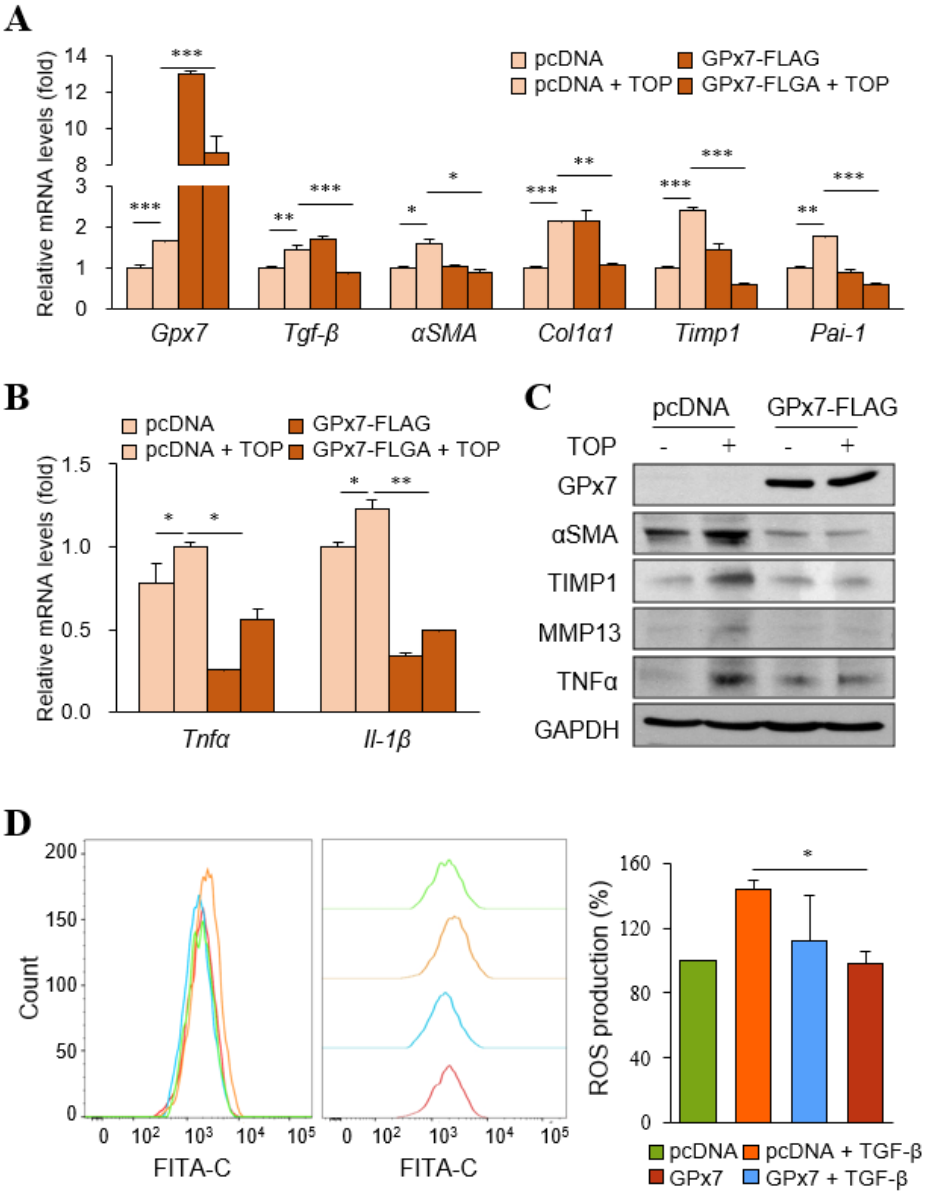

Figure 5. GPx7 ameliorates hepatic fibrosis, inflammation related gene expression in LX-2 cells. (a, b) Relative mRNA expression of indicated genes in LX-2 cells. Cells transfected with the pcDNA3.0 or pcDNA3-GPx7-FLAG vector. (c) Cells transfected with the pcDNA3.0 or pcDNA3-GPx7-FLAG vector. Western blotting analysis using indicated antibodies. GAPDH was used as loading control. (d) ROS production using flow cytometry at GPx7 overexpressed LX-2 cells. All data are presented ± s.d. **P*<0.05, ***P*<0.01, ****P*<0.001.

4. Knockdown of GPx7 accelerates the progression of liver fibrosis in CDAHFD fed mice

To explore whether GPx7 deficiency promotes NASH-fibrosis *in vivo*, I constructed adenovirus containing short hairpin RNA (Ad-shGPx7). 6-week-old mice were fed CDAHFD for three weeks before adenovirus injection. CDAHFD brings an impaired hepatic VLDL secretion, resulting in hepatic inflammation and fibrosis[25]. After 3 weeks, mice were injected Ad-shGPx7 or control virus via tail-vein and after 7 days, mice were sacrificed (Figure 6A). I measured body weight of adenovirus injected mice before virus injection and sacrifice condition. There was not significant change in body weight (Figure 6B). However, liver weight and the ratio of liver to body weight were high in Ad-shGPx7 injected group compared to the control group (Figure 6D). These results also showed in liver tissue. Knockdown group using Ad-shGPx7 had bigger liver tissue compared with control group (Figure 6C). It is indicated that increased liver weights were induced hepatic inflammation and lipid accumulation (Figure 6E-G). These results also showed in fibrosis and inflammation related markers expression (Figure 7A-D). In conclusion, these finding imply that the abundant of GPx7 suppresses NASH-fibrosis through reducing oxidative stress. Using these enzyme activities of GPx7, it can represent a novel therapy for the treatment of NASH-fibrosis.

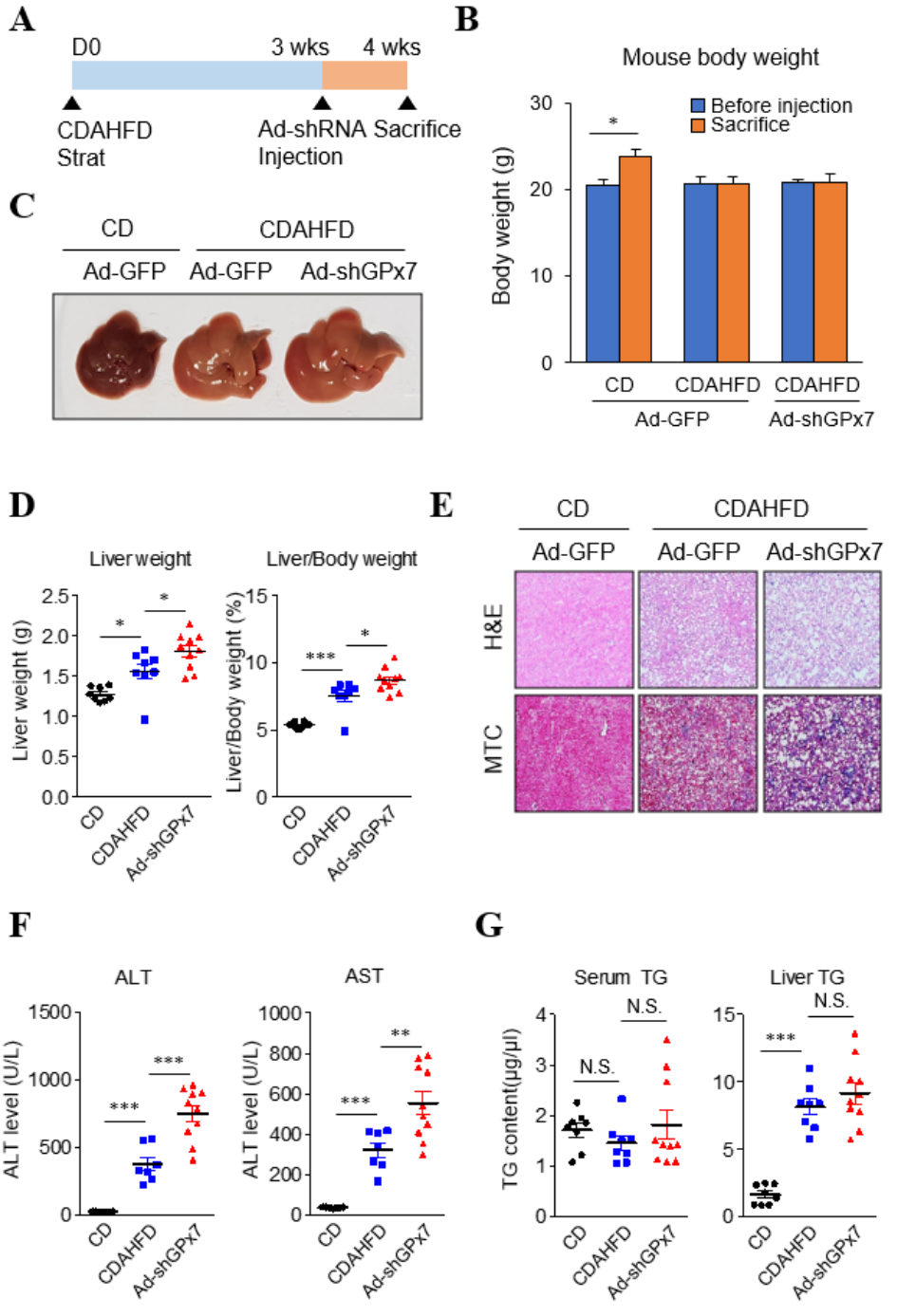

Figure 6. Knockdown of GPx7 induces NASH-fibrosis. (a) Schematic diagram of *in vivo* experiments. (Chow diet, n = 8; CDAHFD group and sh-GPx7 group, n = 10). (b) Body weight changes in mice. (c) Representative liver tissue image. (d) Liver weight and the ratio of liver to body weight in mice. (e) H&E and MTC staining on liver sections from mice. Collagen, blue; muscle fiber, red. (f) Serum ALT and AST level in mice. (g) Serum TG and liver TG level in mice. Black-filled circle, CD + Ad-shControl; Blue-filled square, CDAHFD + Ad-shControl; Red-filled triangle, CDAHFD + Ad-shGPx7. All data are presented ± s.d. **P*<0.05, ***P*<0.01, ****P*<0.001.

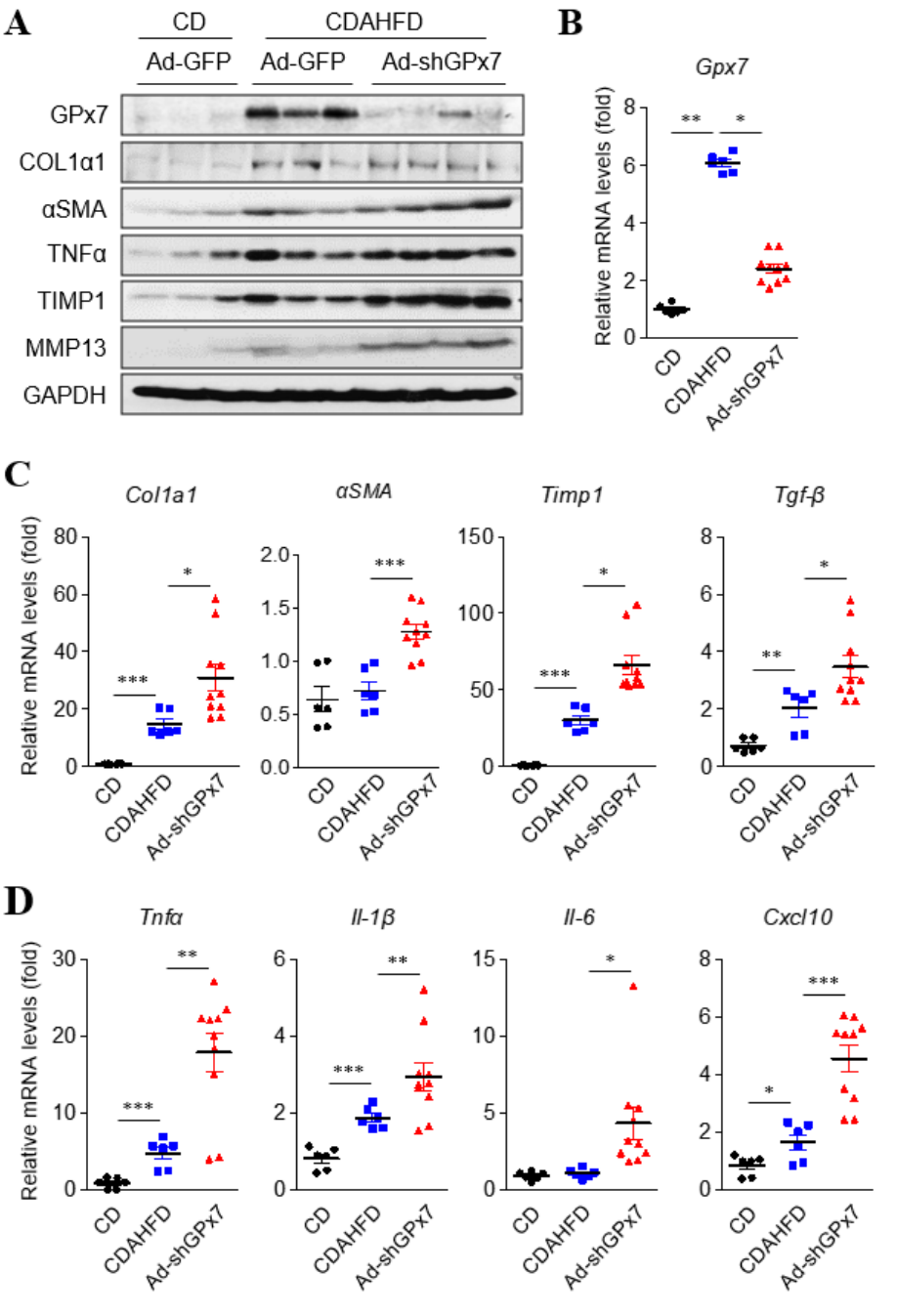

Figure 7. Knockdown of GPx7 increases hepatic inflammation and fibrosis related gene expression. (a) Western blotting analysis using indicated antibodies. GAPDH was used as loading control. (b) Relative mRNA expression of *GPx7*. (c,d) Relative mRNA levels of indicated genes. Black-filled circle, CD + Ad-shControl; Blue-filled square, CDAHFD + Ad-shControl; Red-filled triangle, CDAHFD + Ad-shGPx7. All data are presented ± s.d. **P*<0.05, ***P*<0.01, ****P*<0.001.

IV. DISCUSSION

NASH-fibrosis is the result of chronic liver injury caused by persistent fat accumulation several cytokines through the interaction of HSCs and Kupffer cells, and activated HSCs promote the ECM synthesis [26]. NASH-fibrosis is characterized by excessive collagen accumulation, lobular and portal inflammation, hepatic ballooning and fibrosis [27]. Moreover, NASH-fibrosis plays a role as an indicator of molecular pathological progress to and inflammatory reactions [28]. Liver cell damage triggered by various causes produces hepatocellular carcinoma (HCC) and hepatocytes dysfunction [29]. Thus, the survival rates of chronic liver disease strongly rely on the diagnosis and treatment in NASH-fibrosis, which is the disease before progressing to irreversible cirrhosis. Nevertheless, NASH-fibrosis therapeutic strategy has not been established yet. Therefore, it is important to identify new regulators to develop effective strategies for preventing NASH-fibrosis progression. Here, I found that GPx7 may play an important role during NASH-fibrosis through regulation of liver fibrosis-related gene expression and oxidative stress.

HSCs activation via induction of TGF-β causes NASH-fibrosis by accumulating ECM [30-32]. The high-fat-diet (HFD) is usually used in mice model of liver injury mediated HSC activation [33,34]. In this study, CDAHFD used to induce NASH-fibrosis is composed of 60 kcal% fat and 0.1% methionine, but not containing choline [34]. Although the fat accumulation accompanied by

inflammation and fibrosis is a key characteristic of NASH, serum TG levels had not changed in our result. This is due to CDAHFD inhibits VLDL secretion from liver to serum. However, CDAHFD induced liver TG accumulation in mice and accumulated TG level was not changed by knockdown of GPx7, suggesting GPx7 was not involved in fat accumulation during NASH progression. Given that GPx7 may regulates NASH progression through fibrosis rather than simple steatosis.

Oxidative stress has been reported to play a predominant pro-fibrotic role in liver fibrosis [12,35]. GPx7 has been known as a regulator of ROS-dependent oxidative DNA damage in several cancer types such as gastric and esophageal cancer [23]. However, the exact role of GPx7 in liver disease is not shown. In this study, the antioxidant action of GPx7 in liver was confirmed using NASH-fibrosis model. HSCs activation caused GPx7 overexpression and GPx7 modulated pro-fibrotic gene expression via regulation of intracellular ROS levels. This result indicated that oxidative stress contributes to liver fibrosis during NASH progression, suggesting anti-oxidant may be an alternative therapeutics for NASH-fibrosis.

Overall, my findings demonstrate that GPx7 effectively ameliorates liver fibrogenesis via inhibition of the oxidative stress. GPx7 exhibited a potent anti-fibrotic effect by reducing inflammatory cytokine production, improving pathological changes, and inhibiting ROS production. Taken together, GPx7 overexpression might be as a potential therapeutic target for NASH-fibrosis.

V. CONCLUSION

In summary, the data presented in this report support that a novel gene GPx7 ameliorated NASH-fibrosis through suppressing oxidative stress. In LX-2 cells, knockdown of GPx7 induced fibrosis and inflammation related gene expression, whereas overexpressed GPx7 reduced. Moreover, in CDAHFD fed mice, GPx7 deficiency was deteriorated NASH-fibrosis. To explore the mechanism, I measured ROS production. As a result, GPx7 reduced NASH-fibrosis via inhibiting oxidative stress.

Based on all this research, GPx7 suppresses oxidative stress to prevent liver fibrosis, so using GPx7 enzyme activity can be useful treatment strategy for NASH-fibrosis.

REFERENCES

1. Buzzetti E, Pinzani M, Tsochatzis EA. The multiple-hit pathogenesis of non-alcoholic fatty liver disease (NAFLD). Metabolism 2016;65:1038-48.
2. Hardy T, Oakley F, Anstee QM, Day CP. Nonalcoholic Fatty Liver Disease: Pathogenesis and Disease Spectrum. Annu Rev Pathol 2016;11:451-96.
3. Cohen JC, Horton JD, Hobbs HH. Human fatty liver disease: old questions and new insights. Science 2011;332:1519-23.
4. Szczepaniak LS, Nurenberg P, Leonard D, Browning JD, Reingold JS, Grundy S, et al. Magnetic resonance spectroscopy to measure hepatic triglyceride content: prevalence of hepatic steatosis in the general population. Am J Physiol Endocrinol Metab 2005;288:E462-8.
5. Promrat K, Kleiner DE, Niemeier HM, Jackvony E, Kearns M, Wands JR, et al. Randomized controlled trial testing the effects of weight loss on nonalcoholic steatohepatitis. Hepatology 2010;51:121-9.
6. Huang MA, Greenson JK, Chao C, Anderson L, Peterman D, Jacobson J, et al. One-year intense nutritional counseling results in histological improvement in patients with non-alcoholic steatohepatitis: a pilot study. Am J Gastroenterol 2005;100:1072-81.
7. Chalasani N, Younossi Z, Lavine JE, Diehl AM, Brunt EM, Cusi K, et

al. The diagnosis and management of non-alcoholic fatty liver disease: Practice Guideline by the American Association for the Study of Liver Diseases, American College of Gastroenterology, and the American Gastroenterological Association. 2012;55:2005-23.

8. Sanyal AJ, Chalasani N, Kowdley KV, McCullough A, Diehl AM, Bass NM, et al. Pioglitazone, vitamin E, or placebo for nonalcoholic steatohepatitis. 2010;362:1675-85.

9. Musso G, Cassader M, Rosina F, Gambino RJD. Impact of current treatments on liver disease, glucose metabolism and cardiovascular risk in non-alcoholic fatty liver disease (NAFLD): a systematic review and meta-analysis of randomised trials. 2012;55:885-904.

10. Bjelakovic G, Gluud L, Nikolova D, Bjelakovic M, Nagorni A, Gluud CJAp, et al. Meta-analysis: antioxidant supplements for liver diseases–the Cochrane Hepato-Biliary Group. 2010;32:356-67.

11. Miller ER, Pastor-Barriuso R, Dalal D, Riemersma RA, Appel LJ, Guallar EJAoim. Meta-analysis: high-dosage vitamin E supplementation may increase all-cause mortality. 2005;142:37-46.

12. Gandhi CR. Oxidative Stress and Hepatic Stellate Cells: A PARADOXICAL RELATIONSHIP. Trends Cell Mol Biol 2012;7:1-10.

13. Torok NJ. Dysregulation of redox pathways in liver fibrosis. Am J Physiol Gastrointest Liver Physiol 2016;311:G667-g74.

14. Sanchez-Valle V, Chavez-Tapia NC, Uribe M, Mendez-Sanchez N. Role

of oxidative stress and molecular changes in liver fibrosis: a review. Curr Med Chem 2012;19:4850-60.

15. Nieto N, Friedman SL, Cederbaum AI. Cytochrome P450 2E1-derived reactive oxygen species mediate paracrine stimulation of collagen I protein synthesis by hepatic stellate cells. J Biol Chem 2002;277:9853-64.

16. Yang KL, Chang WT, Hong MY, Hung KC, Chuang CC. Prevention of TGF-beta-induced early liver fibrosis by a maleic acid derivative anti-oxidant through suppression of ROS, inflammation and hepatic stellate cells activation. PLoS One 2017;12:e0174008.

17. McCubrey JA, Lahair MM, Franklin RA. Reactive oxygen species-induced activation of the MAP kinase signaling pathways. Antioxid Redox Signal 2006;8:1775-89.

18. Takada Y, Mukhopadhyay A, Kundu GC, Mahabeleshwar GH, Singh S, Aggarwal BB. Hydrogen peroxide activates NF-kappa B through tyrosine phosphorylation of I kappa B alpha and serine phosphorylation of p65: evidence for the involvement of I kappa B alpha kinase and Syk protein-tyrosine kinase. J Biol Chem 2003;278:24233-41.

19. Bulua AC, Simon A, Maddipati R, Pelletier M, Park H, Kim KY, et al. Mitochondrial reactive oxygen species promote production of proinflammatory cytokines and are elevated in TNFR1-associated periodic syndrome (TRAPS). J Exp Med 2011;208:519-33.

20. Reuter S, Gupta SC, Chaturvedi MM, Aggarwal BB. Oxidative stress, inflammation, and cancer: how are they linked? Free Radic Biol Med 2010;49:1603-16.

21. Yu Y, Sun X, Gu J, Yu C, Wen Y, Gao Y, et al. Deficiency of DJ-1 Ameliorates Liver Fibrosis through Inhibition of Hepatic ROS Production and Inflammation. Int J Biol Sci 2016;12:1225-35.

22. Muthukumar K, Nachiappan V. Cadmium-induced oxidative stress in Saccharomyces cerevisiae. Indian J Biochem Biophys 2010;47:383-7.

23. Chen YI, Wei PC, Hsu JL, Su FY, Lee WH. NPGPx (GPx7): a novel oxidative stress sensor/transmitter with multiple roles in redox homeostasis. Am J Transl Res 2016;8:1626-40.

24. JY Han. Identification of novel genes associated with progression of non-alcoholic fatty liver disease(NAFLD): Yonsei University; 2018.

25. Van Herck MA, Vonghia L, Francque SM. Animal Models of Nonalcoholic Fatty Liver Disease-A Starter's Guide. Nutrients 2017;9.

26. Fujita T, Narumiya S. Roles of hepatic stellate cells in liver inflammation: a new perspective. Inflamm Regen 2016;36:1.

27. Benedict M, Zhang X. Non-alcoholic fatty liver disease: An expanded review. World J Hepatol 2017;9:715-32.

28. Del Campo JA, Gallego P, Grande L. Role of inflammatory response in liver diseases: Therapeutic strategies. World J Hepatol 2018;10:1-7.

29. Lo RC, Kim H. Histopathological evaluation of liver fibrosis and

cirrhosis regression. Clin Mol Hepatol 2017;23:302-7.

30. Higashi T, Friedman SL, Hoshida Y. Hepatic stellate cells as key target in liver fibrosis. Advanced Drug Delivery Reviews 2017;121:27-42.

31. Safadi R, Friedman S. Hepatic fibrosis--role of hepatic stellate cell activation. J MedGenMed: Medscape general medicine 2002;4:27-.

32. Friedman SL, Neuschwander-Tetri BA, Rinella M, Sanyal AJ. Mechanisms of NAFLD development and therapeutic strategies. Nat Med 2018;24:908-22.

33. Zhou Z, Xu MJ, Cai Y, Wang W, Jiang JX, Varga ZV, et al. Neutrophil-Hepatic Stellate Cell Interactions Promote Fibrosis in Experimental Steatohepatitis. Cell Mol Gastroenterol Hepatol 2018;5:399-413.

34. Jing XY, Yang XF, Qing K, Ou-yang Y. Roles of the lipid metabolism in hepatic stellate cells activation big up tri, open. Chin Med Sci J 2013;28:233-6.

35. Novo E, Cannito S, Paternostro C, Bocca C, Miglietta A, Parola M. Cellular and molecular mechanisms in liver fibrogenesis. Arch Biochem Biophys 2014;548:20-37.

ABSTRACT (IN KOREAN)

비 알코올성 지방간질환에서의 GPx7의 기능분석

<지도교수 김 재 우>

연세대학교 대학원 의과학과

김 현 주

비알코올성 지방간질환 (NAFLD)은 전 세계적으로 만성 간질환의 가장 흔한 원인 중 하나이다. NAFLD는 비알코올성 지방간염 (NASH)및 간 경변과 같이 치료가 불가능한 질환으로 진행될 수 있다. 이 연구의 목표는 NAFLD의 진행을 조절하는 분자적 메커니즘을 밝히는 것이다. 이 연구에서는 RNA 시퀀싱을 이용하여 단순 지방증에서와 NASH-fibrosis에서의 유전자 발현을 분석하였다. 그 결과로

GPx7을 발굴해 냈는데, 이는 정상간과 비교하여 NASH-fibrosis 상태에서 유의하게 발현이 증가되었다. siRNA를 사용한 GPx7의 발현 감소는 간섬유증 및 염증을 증가시킨 반면, GPx7의 과발현은 LX-2 세포에서 간섬유증 및 염증 관련 유전자의 발현을 억제하였다. 또한 GPx7이 생체내에서 어떤 역할을 수행하는지 알아보기 위해, 3주간 CDAHFD를 진행한 마우스에 shRNA을 포함하는 아데노바이러스를 주사하였다. GPx7의 발현감소는 간섬유증과, 염증을 유발했다. 이것은 GPx7이 간섬유증의 새로운 조절자가 될 수 있음을 암시한다. NAFLD의 발병기전에는 산화스트레스가 관련되어 있다. GPx7이 산화스트레스 조절에 관여하는지 확인하기 위해, ROS 생산을 측정했다. 이것을 통해 GPx7이 산화 스트레스를 감소시킴으로써 NASH-fibrosis를 개선한다는 것을 알 수 있었다. 종합하면, 이러한 결과는 GPx7이 산화스트레스를 완화시켜 간 섬유증을 예방할 수 있음을 나타낸다. 따라서 GPx7의 효소활성을 활성화시키는 것은 NASH-fibrosis에 대한 유용한 치료 전략이 될 수 있다.

핵심되는 말 : 비 알코올성 지방간 질환, 지방간, 지방간 염증 및 간섬유화, 비알코올성 지방간염, 콜린결핍 아미노산 고지방식이